5-1-2016

Wormhole Geometries in Fourth-Order Conformal Weyl Gravity

Gabriele U. Varieschi
Loyola Marymount University, gvarieschi@lmu.edu

Kellie L. Ault
Loyola Marymount University

Recommended Citation

Gabriele U. Varieschi and Kellie L. Ault, *Int. J. Mod. Phys. D* **25**, 1650064 (2016) [15 pages] DOI:http://dx.doi.org/10.1142/S0218271816500644

Wormhole geometries in fourth-order conformal Weyl gravity

Gabriele U. Varieschi

*Department of Physics, Loyola Marymount University - Los Angeles, CA 90045, USA**

Kellie L. Ault

Department of Physics, Loyola Marymount University - Los Angeles, CA 90045, USA†

Abstract

We present an analysis of the classic wormhole geometries based on conformal Weyl gravity, rather than standard general relativity. The main characteristics of the resulting traversable wormholes remain the same as in the seminal study by Morris and Thorne, namely, that effective super-luminal motion is a viable consequence of the metric.

Improving on previous work on the subject, we show that for particular choices of the shape and redshift functions the wormhole metric in the context of conformal gravity does not violate the main energy conditions at or near the wormhole throat.

Some exotic matter might still be needed at the junction between our solutions and flat spacetime, but we demonstrate that the averaged null energy condition (as evaluated along radial null geodesics) is satisfied for a particular set of wormhole geometries.

Therefore, if fourth-order conformal Weyl gravity is a correct extension of general relativity, traversable wormholes might become a realistic solution for interstellar travel.

PACS numbers: 04.50.Kd; 04.20.Jb; 04.20.Gz

Keywords: conformal gravity, traversable wormholes, super-luminal travel

* Email: gvarieschi@lmu.edu

† Email: kault@lion.lmu.edu

Contents

I. INTRODUCTION

Lorentzian wormholes are essentially shortcuts through space and time; they can either connect two distant regions of our universe or connect our universe with another, totally different one. In 1988 Morris and Thorne [1] introduced a new class of *traversable wormholes* (TW, in the following) that, in principle, can be used for rapid interstellar travel by advanced civilizations. Their solutions were entirely based on standard General Relativity (GR) and represented a substantial improvement over previous wormhole geometries, e.g., Schwarzschild wormholes, Wheeler wormholes, and Kerr wormholes. For general reviews of Lorentzian wormholes see Refs. [2] and [3].

However, even these improved TW solutions possess troublesome features ([1], [4], [5]): they violate the main energy conditions for the stress-energy tensor and they can also be converted into time machines, thus possibly violating causality. The first of these two

problems can only be addressed by invoking the existence of exotic matter, i.e., matter with negative energy density placed at or near the wormhole throat. Although some special effects in quantum field theory (such as the Casimir effect, squeezed vacuum, and others) might allow for the existence of exotic matter, the manifest violation of the energy conditions greatly reduces the possibility to use traversable wormholes for actual interstellar travel.

Notwithstanding these difficulties, progress has been made for wormholes in a GR setting: attempts at self-consistently supporting wormholes with quantum fields have been made ([6], [7]) and classical fields as exotic matter have also been considered (see [8], [9], and rebuttal [10]).

In recent decades, several alternative theories of gravity have been introduced and applied to cosmological models [11] with the advantage of avoiding some of the most controversial elements of standard cosmology—e.g., dark matter, dark energy, and the cosmological constant. In particular, fourth-order Conformal Weyl Gravity (CG, for short, in the following) is a natural extension of Einstein's GR, originally introduced by H. Weyl [12], revisited by P. Mannheim et al. ([13], [14], [15], [16]), and even considered by G. 't Hooft ([17], [18], [19], [20]) as a possible key towards a complete understanding of physics at the Planck scale.

A similar, but different approach to conformal gravity and cosmology has been proposed by one of us in a series of papers ([21], [22], [23], [24], [25], [26]). A new model was introduced that was called kinematical conformal cosmology [21] since it was based on purely kinematic considerations without using any dynamical equation of state for the universe. This model is able to account for the accelerated expansion of the universe ([22], [26]) and may also explain the origin of some gravitational anomalies, such as the Flyby Anomaly [25].

One of these papers [24] studied in detail the implications of CG in relation to the Alcubierre *warp drive* metric [27], which is another well-known theoretical mechanism allowing, in principle, for super-luminal motion, i.e., faster-than-light travel. It was shown [24] that, for particular choices of the warp drive shaping function, the main energy conditions are not violated by the warp drive solutions within the framework of conformal gravity.

Continuing along this line of investigation, the main objective of this paper is to apply CG to traversable wormhole geometries and analyze the related energy conditions and other characteristics of the resultant solutions. Some work on the subject already exists in the literature ([28], [29]), showing that in some cases the energy conditions are not violated. We propose to find more general wormhole solutions, which do not violate the energy conditions

in CG, at least in the vicinity of the wormhole throat. The same problem has been studied with regard to other alternative theories of gravity (for example, see [30], [31], [32], [33], [34], [35]), but in this paper we will limit our analysis to fourth-order conformal Weyl gravity.

In Sect. II, we start with a brief description of the CG field equations and the general form of the CG stress-energy tensor; in Sect. III, we review the standard TW geometry and the related form of the stress energy tensor; in Sect. IV, we describe specific wormhole solutions and analyze the main energy conditions, and, finally, in Sect. V, we present our conclusions.

II. CONFORMAL GRAVITY AND THE STRESS-ENERGY TENSOR

Conformal gravity is based on the Weyl action:[1]

$$I_W = -\alpha_g \int d^4x \, (-g)^{1/2} \, C_{\lambda\mu\nu\kappa} \, C^{\lambda\mu\nu\kappa}, \tag{1}$$

where $g \equiv \det(g_{\mu\nu})$, $C_{\lambda\mu\nu\kappa}$ is the conformal (or Weyl) tensor, and α_g is the CG coupling constant. I_W is the unique general coordinate scalar action that is invariant under local conformal transformations: $g_{\mu\nu}(x) \rightarrow e^{2\alpha(x)} g_{\mu\nu}(x) = \Omega^2(x) g_{\mu\nu}(x)$. The factor $\Omega(x) = e^{\alpha(x)}$ determines the amount of local stretching of the geometry, hence the name conformal for a theory invariant under all local stretchings of the space-time (see [21] and references therein for more details).

This conformally invariant generalization of GR was found to be a fourth-order theory, as opposed to the standard second-order General Relativity, since the field equations contained derivatives up to the fourth order of the metric with respect to the space-time coordinates. These field equations were introduced by R. Bach [37], in the presence of a stress-energy tensor[2] $T_{\mu\nu}$, as follows:

$$W_{\mu\nu} = \frac{1}{4\alpha_g} \, T_{\mu\nu}, \tag{2}$$

[1] In this paper we adopt a metric signature $(-,+,+,+)$ and we follow the sign conventions of Weinberg [36]. In this section we will leave fundamental constants, such as c and G, in all equations, but later we will use geometrized units ($c = 1$, $G = 1$).

[2] We follow here the convention [15] of introducing the stress-energy tensor $T_{\mu\nu}$ so that the quantity cT_{00} has the dimensions of an energy density.

as opposed to Einstein's standard equations,

$$G_{\mu\nu} = R_{\mu\nu} - \frac{1}{2} g_{\mu\nu}\ R = -\frac{8\pi G}{c^3}\ T_{\mu\nu}, \tag{3}$$

where the Bach tensor $W_{\mu\nu}$ is the equivalent in CG of the Einstein curvature tensor $G_{\mu\nu}$ on the left-hand side of Eq. (3).

$W_{\mu\nu}$ has a very complex structure and can be defined in a compact way as:

$$W_{\mu\nu} = 2C^{\alpha}{}_{\mu\nu}{}^{\beta}{}_{;\beta;\alpha} + C^{\alpha}{}_{\mu\nu}{}^{\beta}\ R_{\beta\alpha}, \tag{4}$$

or in an expanded form as:

$$\begin{aligned} W_{\mu\nu} = &-\frac{1}{6} g_{\mu\nu}\ R^{;\lambda}{}_{;\lambda} + \frac{2}{3} R_{;\mu;\nu} + R_{\mu\nu}{}^{;\lambda}{}_{;\lambda} - R_{\mu}{}^{\lambda}{}_{;\nu;\lambda} - R_{\nu}{}^{\lambda}{}_{;\mu;\lambda} + \frac{2}{3} R\ R_{\mu\nu} \\ &- 2R_{\mu}{}^{\lambda}\ R_{\lambda\nu} + \frac{1}{2} g_{\mu\nu}\ R_{\lambda\rho}\ R^{\lambda\rho} - \frac{1}{6} g_{\mu\nu}\ R^2, \end{aligned} \tag{5}$$

involving derivatives up to the fourth order of the metric with respect to space-time coordinates.

Therefore, in CG, the stress-energy tensor is computed by combining together Eqs. (2) and (5):

$$\begin{aligned} T_{\mu\nu} = 4\alpha_g\ W_{\mu\nu} = 4\alpha_g\ (&-\frac{1}{6} g_{\mu\nu}\ R^{;\lambda}{}_{;\lambda} + \frac{2}{3} R_{;\mu;\nu} + R_{\mu\nu}{}^{;\lambda}{}_{;\lambda} - R_{\mu}{}^{\lambda}{}_{;\nu;\lambda} - R_{\nu}{}^{\lambda}{}_{;\mu;\lambda} \\ &+ \frac{2}{3} R\ R_{\mu\nu} - 2R_{\mu}{}^{\lambda}\ R_{\lambda\nu} + \frac{1}{2} g_{\mu\nu}\ R_{\lambda\rho}\ R^{\lambda\rho} - \frac{1}{6} g_{\mu\nu}\ R^2). \end{aligned} \tag{6}$$

This general form of the tensor will be used in the following sections, in connection with the wormhole metric, to compute energy densities, pressures, and other relevant quantities.

In the original papers by Mannheim and Kazanas ([13], [14]), and in the CG wormhole analysis by F. Lobo [28], the computation of the non-zero components of $W_{\mu\nu}$ was done indirectly by differentiating the Weyl action I_W and using Bianchi and trace identities. In contrast, in this work, we compute all the relevant tensors directly from their definitions, using a specialized Mathematica program, which was developed by one of us for a previous study of the warp drive in CG [24].

In particular, this program can compute the conformal tensor $C_{\lambda\mu\nu\kappa}$ in Eq. (1), the Bach tensor $W_{\mu\nu}$ in Eq. (5), and the stress-energy tensor $T_{\mu\nu}$ in Eq. (6), by performing all the

necessary covariant derivatives. To ensure the reliability of the results obtained with our program regarding wormhole geometries, we have reproduced all the results discussed in the CG wormhole analysis by F. Lobo [28], obtaining a perfect agreement.

III. TRAVERSABLE WORMHOLES AND CONFORMAL GRAVITY

A. General form of the metric

The standard metric for traversable wormholes ([1], [2]) can be written in two general forms. In terms of the proper radial distance l ($c = 1$, in the following):

$$ds^2 = -e^{2\Phi(l)}dt^2 + dl^2 + r^2(l)\ \left[d\theta^2 + \sin^2\theta\ d\phi^2\right], \tag{7}$$

where l covers the entire range $(-\infty, +\infty)$, $l = 0$ corresponds to the wormhole throat, and two asymptotically flat regions occur at $l = \pm\infty$. Additional conditions [2] need to be obeyed by the two functions $\Phi(l)$ and $r(l)$; in particular, $\Phi(l)$ needs to be finite everywhere in order to avoid the existence of event horizons.

A more efficient way to express the TW metric is to employ Schwarzschild coordinates $(t,\, r,\, \theta,\, \phi)$:

$$ds^2 = -e^{2\Phi(r)}dt^2 + \frac{dr^2}{1 - b(r)/r} + r^2\ \left[d\theta^2 + \sin^2\theta\ d\phi^2\right], \tag{8}$$

where now $\Phi(r)$ and $b(r)$ are two arbitrary functions of r, respectively called the redshift and the shape function. The wormhole throat corresponds to a minimum value of the radial coordinate, usually denoted by b_0 or r_0 in the literature, so that two coordinate patches are now required, each covering the range $[b_0, +\infty)$, one for the upper universe and one for the lower universe.[3]

The TW metric was originally introduced in 1973 by H. Ellis [38] as the *drainhole* metric:

$$ds^2 = -dt^2 + dl^2 + r^2(l)\ \left[d\theta^2 + \sin^2\theta\ d\phi^2\right], \tag{9}$$

[3] The redshift function $\Phi(r)$ and the shape function $b(r)$ may actually be different on the upper and lower portions of the wormhole (in this case, they are denoted by $\Phi_\pm(r)$ and $b_\pm(r)$). In this paper, we will assume complete symmetry between the upper and lower parts of the wormhole, thus we will need only one function $\Phi(r)$ and only one function $b(r)$ over the range $[b_0, +\infty)$.

corresponding to a special case of the general form in Eq. (7), for $\Phi(l) = 0$ and $r(l) = \sqrt{b_0^2 + l^2}$. This metric was later re-introduced and generalized by Morris-Thorne [1] in 1988, used as a tool for teaching general relativity by J. Hartle [39], visualized in various environments by Müller et al. [40], and recently revisited by Thorne et al. [41] after being popularized by the science fiction movie *Interstellar*.

The arbitrary functions $\Phi(r)$ and $b(r)$ in Eq. (8) also need to satisfy certain conditions (see full details in [1], or [2]) in order to obtain a viable TW solution. The main condition for the redshift function is, again, the requirement for $\Phi(r)$ to be finite everywhere to avoid the presence of event horizons.

The main conditions for the $b(r)$ function are related to the shape of the wormhole, determined by the mathematics of embedding: we need $b(r = b_0) = b_0$ at the throat, $b(r) < r$ away from the throat, and the so-called flaring-out condition [1],

$$\frac{d^2r}{dz^2} = \frac{b(r) - b'(r)\, r}{2b^2(r)} > 0, \tag{10}$$

at or near the throat. The function $r = r(z)$, or $z = z(r)$, determines the profile of the embedding diagram of the wormhole:

$$z(r) = \pm \int_{b_0}^{r} \frac{dr}{\sqrt{\frac{r}{b(r)} - 1}}; \tag{11}$$

the complete embedding diagram is obtained by rotating the graph of the function $z(r)$ around the vertical z-axis.

B. Energy conditions

In a suitable orthonormal frame, the stress-energy tensor assumes a diagonal form, $T^{\widehat{\mu\nu}} = diag(\rho, p_1, p_2, p_3)$, where ρ is the energy density, and p_1, p_2, p_3 are the three principal pressures.

In the case of the wormhole metric of Eq. (8), the spherical symmetry of the metric implies $p_2 = p_3$, so that the stress-energy tensor becomes

$$T^{\widehat{\mu\nu}} = diag(\rho, p_r, p_l, p_l), \tag{12}$$

where p_r indicates the pressure in the radial direction[4] and p_l indicates the pressure in the lateral (θ or ϕ) directions.

The main energy conditions [42] such as the null, weak, strong, and dominant energy conditions (respectively, NEC, WEC, SEC, and DEC in the following) for the stress-energy tensor in Eq. (12), can be expressed directly in terms of ρ, p_r, p_l as follows ([2], [43]):

$$\begin{aligned} NEC &\Longleftrightarrow \quad \rho + p_r \geq 0 \text{ and } \rho + p_l \geq 0 \\ WEC &\Longleftrightarrow \qquad NEC \text{ and } \rho \geq 0 \\ SEC &\Longleftrightarrow \quad NEC \text{ and } \rho + p_r + 2p_l \geq 0 \\ DEC &\Longleftrightarrow \qquad \rho \geq |p_r| \text{ and } \rho \geq |p_l| \,. \end{aligned} \tag{13}$$

In the context of GR, the analysis of the traversable wormhole geometry has shown ([1], [2]) that the NEC is violated over a finite range in the vicinity of the wormhole throat, thus implying violation of the WEC, SEC, and DEC over the same range. At the throat ($r = b_0$), the weaker inequality $[\rho(b_0) + p_r(b_0)] \leq 0$ holds, thus implying that the NEC is violated, or almost violated. Moreover, the topological censorship theorem [44] has shown that GR does not allow an observer to probe the topology of spacetime, thus implying that traversable wormholes require a violation of the averaged null energy condition (ANEC). In any case, exotic matter, defined as violating either the NEC or the WEC, must be threading the wormhole throat in all possible cases in GR.

In CG, the situation might be different because of the different computation of the stress-energy tensor using Eq. (6), instead of Eq. (3). Also, as pointed out in Sect. II.B of Ref. [28], the CG analysis of the energy conditions might require reconsidering the Raychaudhuri equation and its connection with the topological censorship theorem [44] and the ANEC [2].

It is beyond the scope of our current work to analyze the CG equivalent of the topological censorship theorem and the role of the averaged energy conditions, such as the ANEC. Therefore, in our current study, we will just take the energy conditions in Eq. (13) at face value as was ultimately done also in the same Ref. [28]. In addition, in Sect. IV we will simply check numerically the ANEC for the geometries being considered.

As already mentioned in Sect. II, the rather cumbersome computation of the stress-energy

[4] The radial tension τ is often used instead of the radial pressure p_r, i.e., $\tau = -p_r$, especially when τ is a positive quantity, such as in the case of wormholes in GR. In this paper, we prefer to use the radial pressure p_r, since this quantity will be positive for most CG wormholes analyzed in Sect. IV.

tensor has been performed by using our specialized CG Mathematica program. Starting from the TW metric in Eq. (8), all the relevant CG tensors were first evaluated in coordinate basis, then transformed into the more convenient orthonormal basis.

In this basis, there is no difference between covariant and contravariant forms of the stress-energy tensor; therefore, we have:

$$\begin{aligned} \rho &= T^{\widehat{tt}} = T_{\widehat{tt}} \\ p_r &= T^{\widehat{rr}} = T_{\widehat{rr}} \\ p_l &= T^{\widehat{\theta\theta}} = T_{\widehat{\theta\theta}} = T^{\widehat{\phi\phi}} = T_{\widehat{\phi\phi}}. \end{aligned} \tag{14}$$

The full expressions for ρ, p_r, and p_l, as a function of $\Phi(r)$ and $b(r)$, are rather long and will be presented in the Appendix (Sect. VI). In the particular case of $\Phi(r) = 0$ (the so-called zero-tidal-force solutions [1]), the simplified expressions are the following:

$$\begin{aligned} \rho &= \frac{\alpha}{3r^6}\left\{r^2\left[-4r^2b^{(3)} + 8rb'' + b'\left(2rb'' - 5b' - 8\right)\right] + 2rb\left[9b' + r\left(2rb^{(3)} - 5b''\right)\right] - 9b^2\right\} \\ p_r &= \frac{\alpha}{3r^6}\left\{r^2\left[-4rb'' - \left(b' - 8\right)b'\right] + 2rb\left(2rb'' - 3b'\right) + 3b^2\right\} \\ p_l &= \frac{\alpha}{3r^6}\left\{r^2\left[-2r^2b^{(3)} + 6rb'' + b'\left(rb'' - 2b' - 8\right)\right] + rb\left[12b' + r\left(2rb^{(3)} - 7b''\right)\right] - 6b^2\right\}, \end{aligned} \tag{15}$$

where the first two expressions for ρ and p_r are equivalent to those of Eqs. (28)-(29) in Ref. [28].[5]

IV. SPECIFIC CASES AND RELATED ENERGY CONDITIONS

In the previous sections, we discussed at length the general connections between TW geometries and conformal Weyl gravity. In this section, we analyze specific cases for different choices of the functions $\Phi(r)$ and $b(r)$, with the aim of finding solutions which do not violate the energy conditions in the vicinity of the throat.

In general, different strategies can be used to find suitable functions $\Phi(r)$ and $b(r)$: one can start by choosing simple algebraic expressions for Φ and b, as was done for example in

[5] In Ref. [28], the quantity $4\alpha_g$, from Eq. (6), is set to one. In this paper, we prefer to leave this quantity in all our general formulas, such as Eqs. (15), and (A.1)-(A.3).

Refs. [1] and [28], which lead to wormholes with the desired geometries. In this case, one must also make sure that the chosen functions satisfy the additional conditions mentioned in Sect. III A, e.g., the flaring-out condition in Eq. (10).

An alternative strategy is to start with a well-designed shape of the wormhole, given by the profile of the embedding diagram $z = z(r)$, and then use Eq. (11) to determine the related shape function $b(r)$. This was the case, for example, of the recent study by Thorne et al. [41], where a particular geometry with three free shaping parameters (Dneg—Double Negative wormhole) was used to visualize the wormhole.

In this work, we prefer the former approach to the choice of the shape and redshift functions. In an effort to generalize the different forms for b The above figureand Φ existing in the literature, we considered the following functions:

$$b(r) = b_0 \left[(1+\gamma) \left(\frac{b_0}{r} \right)^l - \gamma \left(\frac{b_0}{r} \right)^m \right] \tag{16}$$
$$\Phi(r) = \left[(1-\delta) \left(\frac{b_0}{r} \right)^p - \delta \left(\frac{b_0}{r} \right)^q \right],$$

where γ, l, m, δ, p, and q can be considered as free parameters.

Both functions are made of simple power terms of the ratio b_0/r, similar to those used in the cited literature ([1], [28]). The $b(r)$ function correctly reduces to b_0 for $r = b_0$, and the $\Phi(r)$ function is finite for $r \geq b_0$. The energy conditions in Eq. (13) and the flaring-out condition in Eq. (10) will be satisfied for certain particular ranges of values of the six free parameters in the CG case.

Our Mathematica program allowed us to find these particular values for the free parameters, satisfying the energy conditions in CG. We combined the general CG equations shown in the Appendix for ρ, p_r, and p_l (Eqs. A.1-A.3) together with the expressions in Eq. (16). Then, we computed all the quantities in the energy conditions of Eq. (13) plus the flaring-out condition of Eq. (10). The results thus obtained were plotted as a function of the six free parameters and several solutions were found, satisfying the energy conditions at and near the throat. We present some of these solutions in the following subsections.

A. Solutions with $\Phi = 0$

The simplest class of solutions is obtained by setting the redshift function to zero, i.e., $\Phi(r) = 0$. As already mentioned above, these are also called zero-tidal-force solutions [1] because no radial tidal acceleration is felt by travelers crossing the wormhole. This class of solutions is also obtained by setting $p = q = 0$ and $\delta = 1/2$ in the second line of Eq. (16) above. In this case, we are left with the choice of the three free parameters, γ, l, and m, for the shape function $b(r)$ in the first line of Eq. (16).

By setting $\gamma = 0$ or $\gamma = -1$, the function $b(r)$ reduces to a single power term. Inspection of the graphs of the energy and flaring-out conditions shows that no valid solutions exist in this case: either the NEC is violated, or the flaring-out condition is violated, or both. The same happens for values of γ in the range $-1 < \gamma < 0$.

In contrast, valid solutions can be obtained for $\gamma > 0$, or $\gamma < -1$, by adjusting the values of the remaining parameters l and m. Since all these solutions are similar to each other, in Fig. 1 we present one particular example for $\gamma = 1$, $l = 3$, and $m = 6.5$, which illustrates well these types of solutions. However, we remark that infinitely many other valid solutions can be obtained by adjusting the free parameters within the allowed ranges; the case presented here is by no means unique.

In Fig. 1, we show all the functions related to the energy conditions in Eq. (13) and the flaring-out condition in Eq. (10) for the $b(r)$ function with parameters $\gamma = 1$, $l = 3$, and $m = 6.5$ (for $\Phi = 0$). In this figure, we also set $b_0 = 1$, so that $r \geq 1$, and the (currently unknown) value of the conformal coupling constant α is also set to unity.

We can see immediately that all the plotted energy functions are positive at and near the throat (in the range $1 \leq r \lesssim 1.03$), as evidenced also by the shaded areas (light green—positive; light red—negative); in addition, the flaring-out condition is also satisfied for all values or r. Therefore, for this case, all the main energy conditions—NEC, WEC, SEC, and DEC— are satisfied in the vicinity of the throat, and no exotic matter is needed in this region, as opposed to the GR case.

The wormhole geometry related to this solution will need to be matched to either a flat spacetime, or to the standard CG vacuum solution [13], at about $r \simeq 1.03$ in order to avoid exotic matter beyond this value of the radial coordinate. This can be accomplished by applying appropriate junction conditions as in the case of GR [45].

However, when we tried to match our solutions with $\Phi(r) = 0$ to flat spacetime in several different ways using our Mathematica routines (with either a discontinuous or a smooth transition of the $b(r)$ function into flat spacetime at $r = 1.03$), it was found that some exotic matter needed to be present at the junction. At this point, we are unable to ascertain whether the presence of exotic matter at the junction can be avoided by using a different shape function $b(r)$ or if this is a general feature of all wormhole geometries in CG.

In relation to the already mentioned topological censorship theorem [44] and the violation in GR of the averaged null energy condition, it is interesting to evaluate the ANEC for our wormhole geometries, at least for radial null geodesics denoted by Γ in the following. For this case, it is sufficient to evaluate the ANEC integral (see Ref. [2], Sect. 12.4.2 and Eq. 12.63):

$$I_\Gamma = \int_{l=-\infty}^{l=+\infty} \left[\rho(l) - \tau(l)\right] e^{-\Phi(l)} dl = 2 \int_{r=b_0}^{r=\infty} \frac{\left[\rho(r) + p_r(r)\right] e^{-\Phi(r)}}{\sqrt{1 - b(r)/r}} dr. \tag{17}$$

This integral is first expressed as a function of the proper radial distance l used in the metric of Eq. (7), then converted into the radial coordinate r by using the connection $dl = \pm \frac{dr}{\sqrt{1-b(r)/r}}$, for the upper and lower parts of the wormhole respectively. We also used the relation $\tau = -p_r$, see footnote after Eq. (12).

We computed numerically the ANEC integral in Eq. (17) for the class of $\Phi = 0$ solutions considered in this subsection for different values of the parameters γ, l, and m in Eq. (16), always obtaining negative results. Thus, the ANEC is violated for specific cases of this class of wormhole geometries (in particular, for $b_0 = 1$, $\alpha = 1$, $\gamma = 1$, $l = 3$, and $m = 6.5$ we obtained $I_\Gamma = -6.35$ cm^{-1}). This suggests that the violation is a generic feature of this class of geometries. In contrast, positive results of the ANEC integral will be obtained for the class of $\Phi \neq 0$ solutions described in the next subsection IV B.

In summary, our solutions for the $\Phi = 0$ case, represent a generalization and a definite improvement over the solutions presented in Sect. III. A. of Ref. [28]. In this reference, the CG solutions for $\Phi = 0$ were either violating all the energy conditions, or were satisfying only the NEC while violating the other conditions. In contrast, we have shown that in CG, it is easy to find a class of solutions, even in the $\Phi = 0$ case, which does not violate any energy condition at or near the throat.

In addition to the solutions presented above, we also tried several other shape functions

different from the one described in Eq. (16). Adding other power terms to the function $b(r)$ does not significantly change the outcome of the analysis: for certain values of the free parameters we obtain valid solutions similar to the ones already described. Starting instead with predefined shapes for the wormhole (such as the Ellis wormhole, the Dneg wormhole, or others), does not yield solutions in CG which satisfy completely the energy conditions; therefore, we will not consider here these other solutions.

B. Solutions with $\Phi \neq 0$

Another class of solutions can be obtained by setting $\Phi \neq 0$, using the special form for Φ in Eq. (16). Again, this particular Φ function generalizes other redshift functions used in the literature, and we adopted a combination of two power terms of the ratio b_0/r in order to keep this function as simple as possible.

It should be noted that for $\delta = 0$ in Eq. (16), the redshift function reduces to $\Phi(r) = (b_0/r)^p$, similar to the one used in Sect. III. B. of Ref. [28] (with $p = 1$), while for $\delta = 1$ the redshift function reduces to $-(b_0/r)^q$, similar to the one used in Sect. III. C. of the same cited reference (with $q = 1$). Our more general choice for $\Phi(r)$ allows us to change the values of the free parameters δ, p, and q, in order to explore all possible cases.

However, after extensive testing of all possible combinations of the parameters, we found that the $\Phi \neq 0$ solutions are not much different from the $\Phi = 0$ solutions studied in the previous subsection, at least energetically. Depending on the values of the six free parameters, we either obtain solutions which satisfy the energy condition up to a certain maximum value for r, or solutions which clearly violate them. The presence of the $\Phi(r)$ term in the metric simply adds some sort of fine-tuning effect to the $\Phi = 0$ solutions, but does not change significantly the analysis of the energy conditions.

For example, Fig. 2 shows one particular solution for the following parameter values: $\delta = 1$, $q = 1$, $\gamma = 1$, $l = 3$, and $m = 5$ (also, $b_0 = 1$ and $\alpha = 1$). Therefore, it is a special case with $\Phi(r) = -(b_0/r)$, similar to the one in Sect. III. C. of Ref. [28]. Once again, the plotted energy functions clearly show that all energy conditions are satisfied in the vicinity of the throat, for $1 \leq r \lesssim 1.10$, and that the flaring-out condition is also satisfied over the whole range of r.

As already discussed in Sect. IV A for the $\Phi = 0$ case, we also matched our $\Phi \neq 0$

solutions described above with flat spacetime at $r = 1.10$ with similar results: some exotic matter is needed at the junction also in the $\Phi \neq 0$ case.

However, the analysis of the ANEC integral in Eq. (17) yields completely different results in this case. Due to the presence of the $e^{-\Phi(r)}$ term in this equation (with $\Phi \neq 0$, in this case), the (numerically integrated) value of the ANEC condition is now *positive* for a wide range of the parameters. In particular, for $b_0 = 1$, $\alpha = 1$, $\delta = 1$, $q = 1$, $\gamma = 1$, $l = 3$, and $m = 5$ (corresponding to the solution presented in Fig. 2), we obtained $I_\Gamma = 5.99$ cm^{-1}. Positive values of the ANEC integral are also obtained if we match our $\Phi \neq 0$ solutions with flat spacetime at $r \simeq 1.10$, with smooth or discontinuous transitions.

Although the ANEC integrals were computed just along radial null geodesics, the positive values obtained in this subsection seem to indicate that the averaged null energy condition is satisfied for our $\Phi \neq 0$ solutions. This suggests that the topological censorship theorem may not apply to conformal gravity.

In figures 3 and 4, we show the actual shape of the wormholes studied above by plotting the standard embedding diagrams for $b_0 = 1$, with the other parameters set as before. These embedding diagrams were obtained by rotating the graph of the function $z(r)$ in Eq. (11) around the vertical z-axis. The correct shape of the wormholes, illustrated in Figs. 3-4, confirms that the flaring-out condition is verified for these solutions.

V. CONCLUSIONS

In this paper, we have analyzed in detail different wormhole geometries within the framework of fourth-order Conformal Weyl Gravity. We have seen that, for particular choices of the shape and redshift functions, we can overcome the main limitation of TW in standard General Relativity, namely, the violation of the energy conditions at or near the throat.

In fact, we have shown that for several different wormhole shapes, the CG solutions do not violate any energy condition in the vicinity of the throat. In particular, this can be achieved even with $\Phi = 0$, zero-tidal-force solutions, unlike previous works in the literature that have only found viable $\Phi \neq 0$ solutions.

Some exotic matter might still be needed at the junction between our solutions and flat spacetime, although more work will be needed to analyze in detail the junction condition formalism in CG. Similarly, the connection between the Raychaudhuri equation, the topolog-

ical censorship theorem, and the ANEC might need to be reconsidered in CG. Our analysis of the ANEC has shown that this condition is likely to be satisfied for our class of $\Phi \neq 0$ wormholes in CG, thus implying that it is qualitatively easier to make traversable wormholes in conformal gravity than in GR.

The TW mechanism might be theoretically feasible if CG is the correct extension of current gravitational theories. All components of the stress-energy tensor can be analytically calculated, using our specialized Mathematica program based on Conformal Gravity. Therefore, traversable wormholes can be, at least in principle, fully engineered following our computations.

VI. APPENDIX: ENERGY DENSITY AND PRESSURE EXPRESSIONS IN CONFORMAL GRAVITY

We present here the general expressions for the energy density ρ, the radial pressure p_r, and the lateral pressure p_l in Conformal Gravity, computed using our specialized Mathematica program from the metric in Eq. (8). These quantities are defined in terms of the arbitrary functions $\Phi(r)$ and $b(r)$, and their derivatives, as follows:

$$
\begin{aligned}
\rho = \frac{\alpha}{3r^6}\{ & r^2[-b'^2(r\,(6r\Phi'' + \Phi'\,(3r\Phi' - 2)) + 5) + 4r(2b'' + r(r\Phi'(b^{(3)} - 4r\Phi^{(3)} - 22\Phi'') \\
& - b^{(3)} + \Phi'^2\,(2r\,(b'' + r\Phi'') - 5) - r(-4b''\Phi'' + 2r\Phi^{(4)} + 8\Phi^{(3)} + 3r\Phi''^2) + r^2\Phi'^4 - 2r\Phi'^3)) \\
& + b'(2r(\Phi'\left(-rb'' + 18r^2\Phi'' - 10\right) + b'' - 2r^2\Phi'^3 + 20r\Phi'^2 + 2r(6r\Phi^{(3)} + 5\Phi'')) - 8)] \\
& - 2rb[b'(r(-2r^2\Phi'^3 + 2\Phi'\left(9r^2\Phi'' - 4\right) + 17r\Phi'^2 + 4r(3r\Phi^{(3)} + \Phi'')) - 9) \\
& + r(4r^2\Phi'^2\,(b'' + 2r\Phi'') + 5b'' - 2r(b^{(3)} - (4rb'' + 5)\,\Phi'' + 4r^2\Phi^{(4)} + 6r^2\Phi''^2 + 10r\Phi^{(3)}) \\
& - \Phi'(r(2r(-b^{(3)} + 8r\Phi^{(3)} + 35\Phi'') + b'') + 10) + 4r^3\Phi'^4 - 10r^2\Phi'^3)] \\
& + b^2[r(4r^3\Phi'^4 - 12r^2\Phi'^3 + r\Phi'^2\left(8r^2\Phi'' + 17\right) - 2r(6r^2\Phi''^2 - 7\Phi'' + 4r(r\Phi^{(4)} + \Phi^{(3)})) \\
& - 2\Phi'(8r^3\Phi^{(3)} + 26r^2\Phi'' + 9)) - 9]\}
\end{aligned}
\tag{A.1}
$$

$$
\begin{aligned}
p_r = \frac{\alpha}{3r^6}\{&8r^4\Phi''[b'\left(1-r\Phi'\right)+r^2\Phi'^2-2] \\
&-r^2\left(r\Phi'-1\right)[4r\left(r\Phi'-1\right)\left(b''+\Phi'\left(r\Phi'-4\right)\right)+b'^2\left(r\Phi'-1\right)+4b'\left(r\Phi'\left(r\Phi'-1\right)+2\right)] \\
&+2rb[2r(-\Phi'(2r(b''+2r^2\Phi^{(3)}-r\Phi'')+5)+r\Phi'^2\left(r\left(b''-4r\Phi''\right)+16\right)+b''+2r^3\Phi'^4 \\
&-11r^2\Phi'^3+2r(\Phi''\left(r^2\Phi''+3\right)+2r\Phi^{(3)}))+b'\left(r\Phi'-1\right)\left(r\left(4r\Phi''+\Phi'\left(2r\Phi'-1\right)\right)+3\right)] \\
&+b^2[r(-4r^3\Phi'^4+20r^2\Phi'^3-4r(\Phi''\left(r^2\Phi''+2\right)+2r\Phi^{(3)})+r\Phi'^2\left(8r^2\Phi''-29\right) \\
&+\Phi'(8r^3\Phi^{(3)}-8r^2\Phi''+6))+3]-4r^6\Phi''^2+8r^5\Phi^{(3)}\left(r\Phi'-1\right)\}
\end{aligned}
\tag{A.2}
$$

$$
\begin{aligned}
p_l = \frac{\alpha}{3r^6}\{&r^2[b'^2\left(-r^2\left(3\Phi''+\Phi'^2\right)-2\right)+2r(3b''+r(-b^{(3)}+\left(3rb''+4\right)\Phi'^2 \\
&-2r(-2b''\Phi''+3\Phi^{(3)}+r(\Phi^{(4)}+\Phi''^2))+\Phi'(r(b^{(3)}-6r\Phi^{(3)}-22\Phi'')-2b'')+2r^2\Phi'^4+4\Phi'' \\
&-8r\Phi'^3))+b'(r(\Phi'\left(-rb''+22r^2\Phi''-4\right)+b''+16r\Phi'^2+6r(2r\Phi^{(3)}+\Phi''))-8)-8r\Phi'] \\
&+rb[r(-2r\left(3rb''+16\right)\Phi'^2-7b''+2r(b^{(3)}-\left(4rb''+11\right)\Phi''+4r^2\Phi^{(4)}+4r^2\Phi''^2+6r\Phi^{(3)}) \\
&+\Phi'(2r^2(-b^{(3)}+12r\Phi^{(3)}+33\Phi'')+5rb''+20)-8r^3\Phi'^4+32r^2\Phi'^3)-2b'(6r^3\Phi^{(3)} \\
&+r\Phi'\left(11r^2\Phi''+7r\Phi'-2\right)-6)]+b^2[r(-4r^3\Phi^{(4)}-4r^3\Phi''^2+4r^3\Phi'^4-16r^2\Phi'^3 \\
&-2\Phi'(6r^3\Phi^{(3)}+11r^2\Phi''+6)+11r\Phi''+23r\Phi'^2)-6]\}
\end{aligned}
\tag{A.3}
$$

Acknowledgments

This work was supported by a grant from the Frank R. Seaver College of Science and Engineering, Loyola Marymount University. The authors would like to thank the anonymous reviewer for the valuable suggestions and useful comments which helped improve the final version of this paper.

---

[1] M. S. Morris and K. S. Thorne, American Journal of Physics **56**, 395 (1988).

[2] M. Visser, *Lorentzian wormholes. From Einstein to Hawking* (American Institute of Physics, Woodbury, N.Y., USA, 1995).

[3] F. S. Lobo (2007), arXiv:0710.4474 [gr-qc].

[4] M. S. Morris, K. S. Thorne, and U. Yurtsever, Physical Review Letters **61**, 1446 (1988).

[5] J. L. Friedman and A. Higuchi, Annalen Phys. **15**, 109 (2006), arXiv:0801.0735 [gr-qc].

[6] D. Hochberg, A. Popov, and S. V. Sushkov, Phys. Rev. Lett. **78**, 2050 (1997), arXiv: gr-qc/9701064.

[7] L. M. Butcher, Phys. Rev. **D90**, 024019 (2014), arXiv:1405.1283 [gr-qc].

[8] C. Barcelo and M. Visser, Phys. Lett. **B466**, 127 (1999), arXiv: gr-qc/9908029.

[9] C. Barcelo and M. Visser, Class. Quant. Grav. **17**, 3843 (2000), arXiv: gr-qc/0003025.

[10] L. M. Butcher, Phys. Rev. **D91**, 124031 (2015), arXiv: 1503.04145 [gr-qc].

[11] T. Clifton, P. G. Ferreira, A. Padilla, and C. Skordis, Phys.Rept. **513**, 1 (2012), arXiv:1106.2476 [astro-ph.CO].

[12] H. Weyl, Math Z. **2**, 384 (1918).

[13] P. D. Mannheim and D. Kazanas, Astrophys. J. **342**, 635 (1989).

[14] D. Kazanas and P. D. Mannheim, Astrophys. J. Suppl. **76**, 431 (1991).

[15] P. D. Mannheim, Prog.Part.Nucl.Phys. **56**, 340 (2006), astro-ph/0505266.

[16] P. D. Mannheim, Foundations of Physics **42**, 388 (2012), arXiv:1101.2186 [hep-th].

[17] G. 't Hooft (2014), arXiv:1410.6675 [gr-qc].

[18] G. 't Hooft (2010), arXiv:1009.0669 [gr-qc].

[19] G. 't Hooft (2010), arXiv:1011.0061 [gr-qc].

[20] G. 't Hooft, Found.Phys. **41** (2011), arXiv:1104.4543 [gr-qc].

[21] G. U. Varieschi, Gen.Rel.Grav. **42**, 929 (2010), arXiv:0809.4729 [gr-qc].

[22] G. U. Varieschi, ISRN Astron.Astrophys. **2011**, 806549 (2011), arXiv:0812.2472 [astro-ph].

[23] G. U. Varieschi, Phys.Res.Int. **2012**, 469095 (2012), arXiv:1010.3262 [astro-ph.CO].

[24] G. U. Varieschi and Z. Burstein, ISRN Astron.Astrophys. **2013**, 482734 (2013), arXiv:1208.3706 [gr-qc].

[25] G. U. Varieschi, Gen.Rel.Grav. **46**, 1741 (2014), arXiv:1401.6503 [gr-qc].

[26] G. Varieschi, Galaxies **2**, 577 (2014), arXiv:1410.2944 [astro-ph.CO].

[27] M. Alcubierre, Class.Quant.Grav. **11**, L73 (1994), arXiv:gr-qc/0009013.

[28] F. S. N. Lobo, Classical and Quantum Gravity **25**, 175006 (2008), arXiv:0801.4401 [gr-qc].

[29] J. Oliva, D. Tempo, and R. Troncoso, International Journal of Modern Physics A **24**, 1528 (2009), arXiv:0907.1128 [hep-th].

[30] J. P. Lemos, F. S. Lobo, and S. Quinet de Oliveira, Phys.Rev. **D68**, 064004 (2003), arXiv:gr-qc/0302049.

[31] C. G. Boehmer, T. Harko, and F. S. Lobo, Phys.Rev. **D76**, 084014 (2007), arXiv:0708.1537 [gr-qc].

[32] F. S. Lobo and M. A. Oliveira, Phys.Rev. **D80**, 104012 (2009), arXiv:0909.5539 [gr-qc].

[33] F. S. N. Lobo, in *American Institute of Physics Conference Series*, edited by J. Beltrán Jiménez, J. A. Ruiz Cembranos, A. Dobado, A. López Maroto, and A. De la Cruz Dombriz (2012), vol. 1458 of *American Institute of Physics Conference Series*, pp. 447–450, arXiv:1112.6333 [gr-qc].

[34] F. S. Lobo, EPJ Web Conf. **58**, 01006 (2013), arXiv:1212.1006 [gr-qc].

[35] T. Harko, F. S. N. Lobo, M. K. Mak, and S. V. Sushkov, Phys. Rev. D **87**, 067504 (2013), arXiv:1301.6878 [gr-qc].

[36] S. Weinberg, *Gravitation and Cosmology: Principles and Applications of the General Theory of Relativity* (Wiley, New York, USA, 1972).

[37] R. Bach, Math Z. **9**, 110 (1921).

[38] H. Ellis, J.Math.Phys. **14**, 104 (1973).

[39] J. Hartle, *Gravity: An introduction to Einstein's general relativity* (Addison Wesley, San Francisco, CA, USA, 2003).

[40] T. Muller, Am.J.Phys. **72**, 1045 (2004).

[41] O. James, E. von Tunzelmann, P. Franklin, and K. S. Thorne, American Journal of Physics **83**, 486 (2015), arXiv:1502.03809 [gr-qc].

[42] S. Hawking and G. Ellis, *The Large Scale Structure of Space-Time* (Cambridge University Press, New York, USA, 1973).

[43] R. Wald, *General relativity* (University of Chicago Press, Chicago, USA, 1984).

[44] J. L. Friedman, K. Schleich, and D. M. Witt, Phys. Rev. Lett. **71**, 1486 (1993), [Erratum: Phys. Rev. Lett.75,1872(1995)], arXiv: gr-qc/9305017.

[45] C. W. Misner, K. S. Thorne, and J. A. Wheeler, *Gravitation* (W.H. Freeman and Co., San Francisco, USA, 1973).

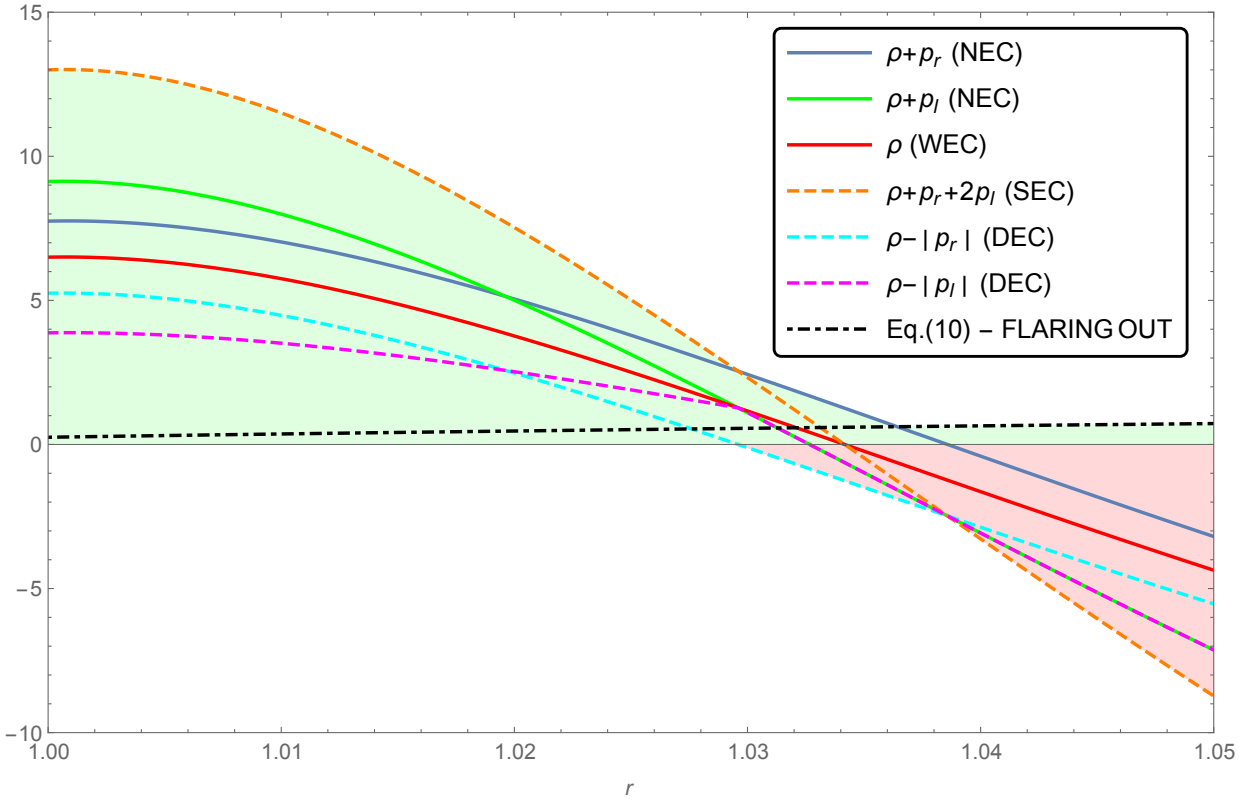

Figure 1: The functions related to the energy conditions in Eq. (13) and the flaring-out condition in Eq. (10) are shown here for a particular shape function with parameters $\gamma = 1$, $l = 3$, and $m = 6.5$ (for $\Phi = 0$). We also set $b_0 = 1$ and $\alpha = 1$. Shaded areas (light green—positive; light red—negative) are used to emphasize regions where the energy conditions are satisfied or violated. All plotted energy functions are positive at and near the throat (in the range $1 \leq r \lesssim 1.03$) showing that no exotic matter is needed in CG as opposed to the GR case.

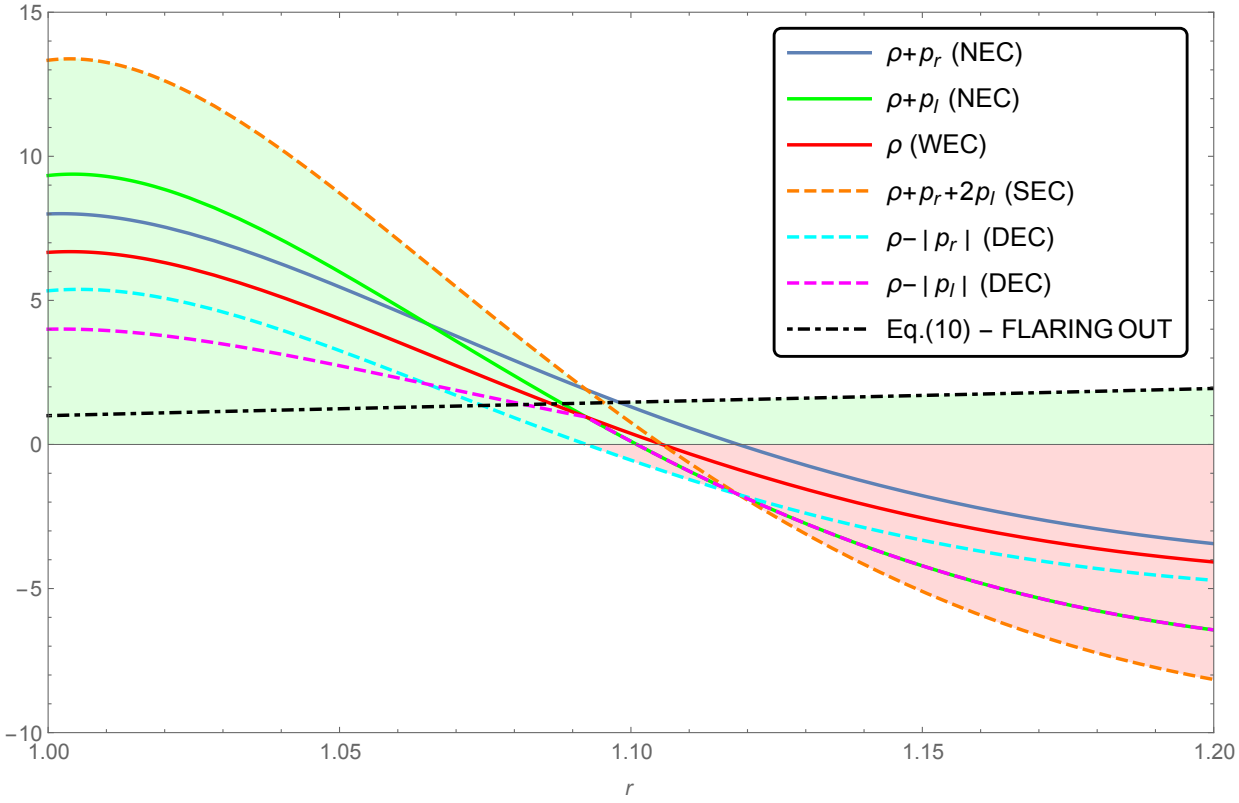

Figure 2: The functions related to the energy conditions in Eq. (13) and the flaring-out condition in Eq. (10) are shown here for a particular shape function with parameters $\delta = 1$, $q = 1$, $\gamma = 1$, $l = 3$, and $m = 5$ ($\Phi \neq 0$ case). We also set $b_0 = 1$ and $\alpha = 1$. Shaded areas (light green—positive; light red—negative) are used to emphasize regions where the energy conditions are satisfied or violated. All plotted energy functions are positive at and near the throat (in the range $1 \leq r \lesssim 1.10$) showing that no exotic matter is needed in CG as opposed to the GR case.

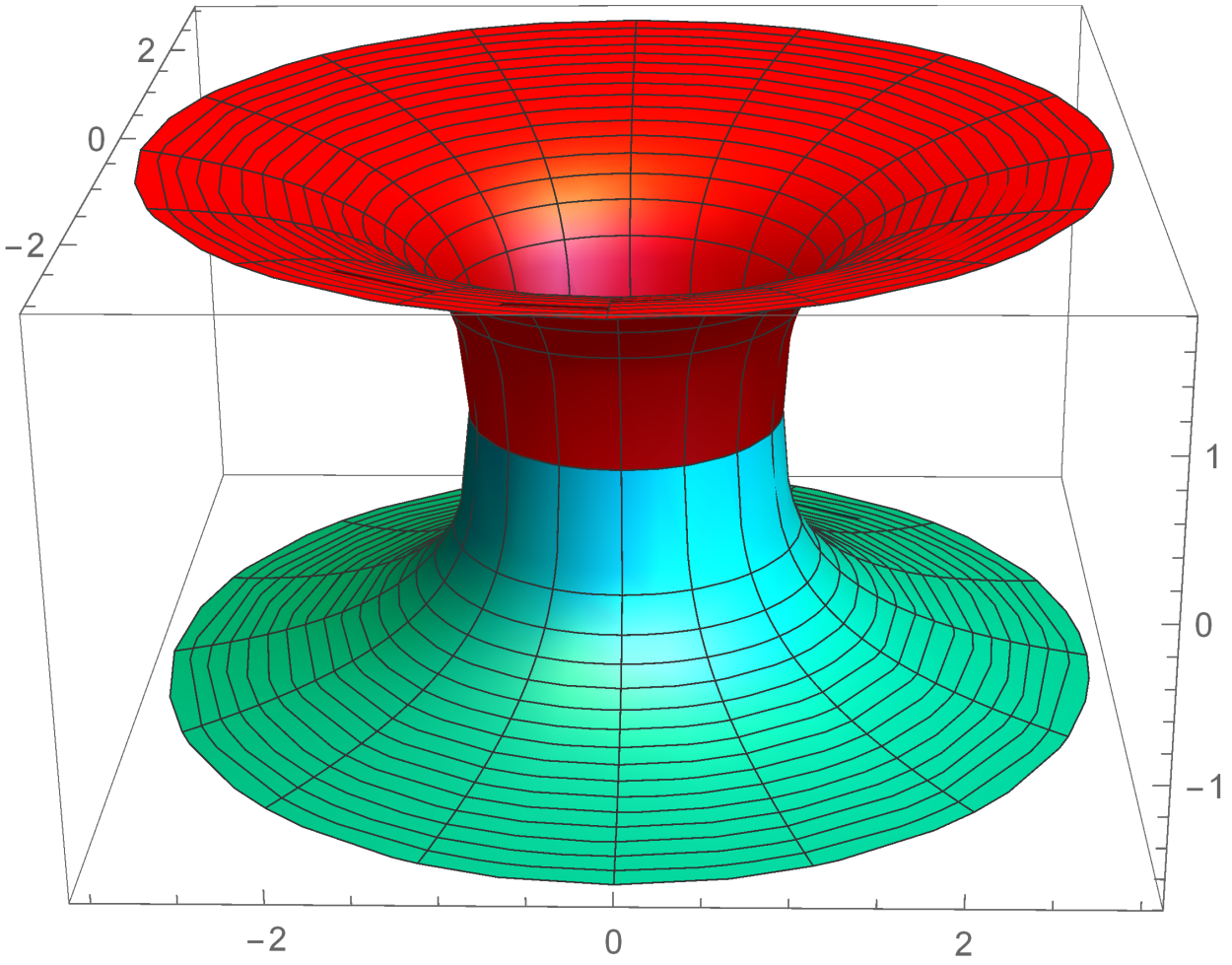

Figure 3: The shape of the wormhole studied in Fig. 1 is illustrated here by plotting the standard embedding diagram for $b_0 = 1$, $\alpha = 1$, and with the other parameters set as before. The shape of the wormhole confirms that the flaring-out condition is verified for this solution (this figure was not included in the published version of the paper).

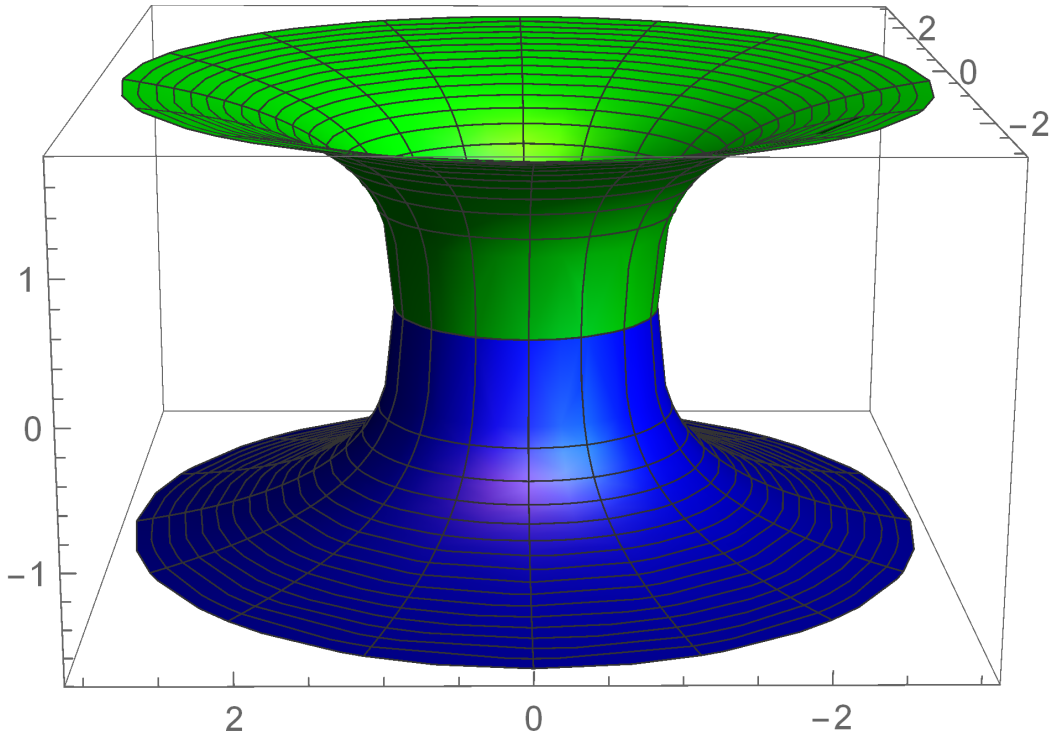

Figure 4: The shape of the wormhole studied in Fig. 2 is illustrated here by plotting the standard embedding diagram for $b_0 = 1$, $\alpha = 1$, and with the other parameters set as before. The shape of the wormhole confirms that the flaring-out condition is verified for this solution (this figure was not included in the published version of the paper).